A Screening-Level HEC-HMS Model for Post-Fire Runoff Emergency Assessment

Taylor S. Cagle, Research Hydraulic Engineer, USACE-ERDC-CHL, Vicksburg, MS, Taylor.S.Cagle@erdc.dren.mil

Stephen W. Brown, Research Hydrologic Engineer, USACE-ERDC-CHL, Vicksburg, MS, Stephen.W.Brown@erdc.dren.mil

Elizabeth A. Shaloka, Hydraulic Engineer, USACE Philadelphia District, Philadelphia, PA, Elizabeth.A.Shaloka@usace.army.mil

Kyle S. Cannon, Student Intern, USACE-ERDC-CHL, Vicksburg, MS, Kyle.S.Cannon@usace.army.mil

Ian E. Floyd, Research Physical Scientist, USACE-ERDC-CHL, Vicksburg, MS, Ian.E.Floyd@erdc.dren.mil

Abstract

Since 2000, wildfires have burned an annual average of 7 million acres, which is more than double the annual acreage burned in the 1990s. Wildfires pose extreme risk to life and property while burning which continues after they are extinguished in the form of elevated flood and debris flow hazards. Changes to the landscape and soil properties after a wildfire, such as the absence of vegetation and the reduction in water infiltration, can cause significant increases in flood magnitude along with the likelihood of dangerous debris flows during post-fire rain events. Hydrologic models help forecast dynamically changing risk to people and infrastructure downstream of burn scars.

In this study, the Hydrologic Engineering Center's Hydrologic Modeling System (HEC-HMS) was used to develop a screening-level model of the South Fork of the Tule River watershed in California for post-fire runoff analysis. Post-fire flood events were simulated for a period after the Windy Fire, which occurred in September of 2021. Simulations of the 1/10, 1/25, and 1/100 AEP floods (10-, 25-, and 100-year storms) were run to estimate changes in peak discharge and post-wildfire debris yield. For the subbasin that experienced the largest percentage of medium to high burn severity (Subbasin 2), model results showed a pre- and post-fire difference in peak discharge of 1,500 cfs, 2,360 cfs, and 4,600 cfs and a post-fire sediment yield of 24,000 tons, 39,000 tons, and 92,000 tons for the 1/10, 1/25, and 1/100 AEP floods, respectively.

Evaluation of model parameterization will help inform future development of screening-level flood risk management models for post-wildfire clear water, sediment, and debris flow simulations to reduce response time in future emergency situations. The data, methods, workflows, and lessons learned during the development of this screening-level hydrologic analysis are currently being tested on additional watersheds. These resulting workflows will be automated to provide a quick starting point for field engineers and scientists who can then apply their regional skill for refined calibration and validation.

Introduction

The United States Army Corps of Engineers (USACE) Engineer Research and Development Center (ERDC) has developed a screening-level HEC-HMS (Hydrologic Engineering Center's Hydrologic Modeling System) model to assess the potential for post-fire debris yield in the Tule River Basin in southern California after the Windy Fire that occurred in 2021. After a wildfire occurs, minimizing the time it takes to complete an emergency response assessment is crucial to reduce the potential for further damage and loss of life due to post-fire runoff events. The development of hydrologic models to inform decision makers of the highest risk regions for debris flows is an important part of this process. HEC-HMS is commonly used in this type of assessment, but accurately parameterizing a debris flow model requires many different methods across multiple disciplines and can take significant time and resources. Having a framework in place that streamlines model development will optimize the response time of this process. This study is intended to help inform engineers and researchers of the simplest and most accurate methods for model parameterization when simulating post-fire runoff events so that a framework can be put in place for more efficient future emergency response assessments.

Background

On September 9, 2021, lightning ignited the Windy Fire that eventually burned 97,528 acres in the Sequoia National Forest area located in southern California (Figure 1). The Tule River Reservation watershed, located in the Northwest portion of the burn perimeter in Tulare County, was one of the areas impacted by the fire (Figure 2). The burned portion of the South Fork Tule River watershed modeled in this study, ranged in severity from unburned to high burn with the majority of the area experiencing a low burn severity (Figure 3). The Windy Fire impacted the headwaters of the Tule River watershed, increasing the chances for post-fire runoff effects to the downstream inhabited areas and thus initiating the need for an emergency response assessment.

Figure 1. Firefighters battling the flames as the Windy Fire burns in the Trail of 100 Giants grove in the Sequoia National Forest, California. (Berger, 2021).

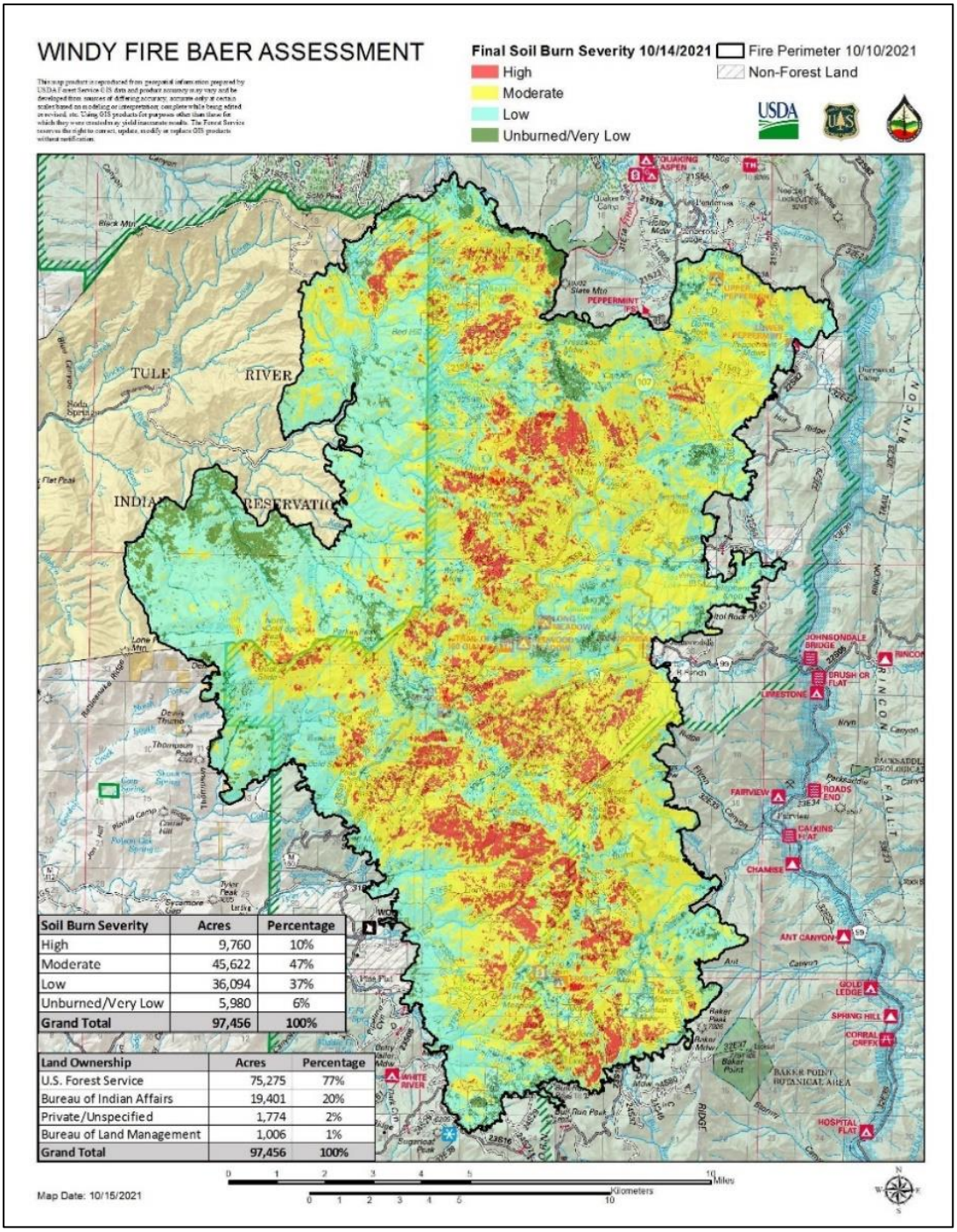

Soil Burn Severity	Acres	Percentage
High	9,760	10%
Moderate	45,622	47%
Low	36,094	37%
Unburned/Very Low	5,980	6%
Grand Total	**97,456**	**100%**

Land Ownership	Acres	Percentage
U.S. Forest Service	75,275	77%
Bureau of Indian Affairs	19,401	20%
Private/Unspecified	1,774	2%
Bureau of Land Management	1,006	1%
Grand Total	**97,456**	**100%**

Figure 2. Shown here is the Windy Fire BARC (Burned Area Reflectance Classification) burn severity map produced by the Burn Area Emergency Response (BAER) Team. Red indicates high burn, yellow indicates moderate burn, blue indicates low burn, and green indicates unburned/very low burn severity. The Tule River watershed can be seen in the Northwest portion of the map indicated by light yellow. (Inciweb)

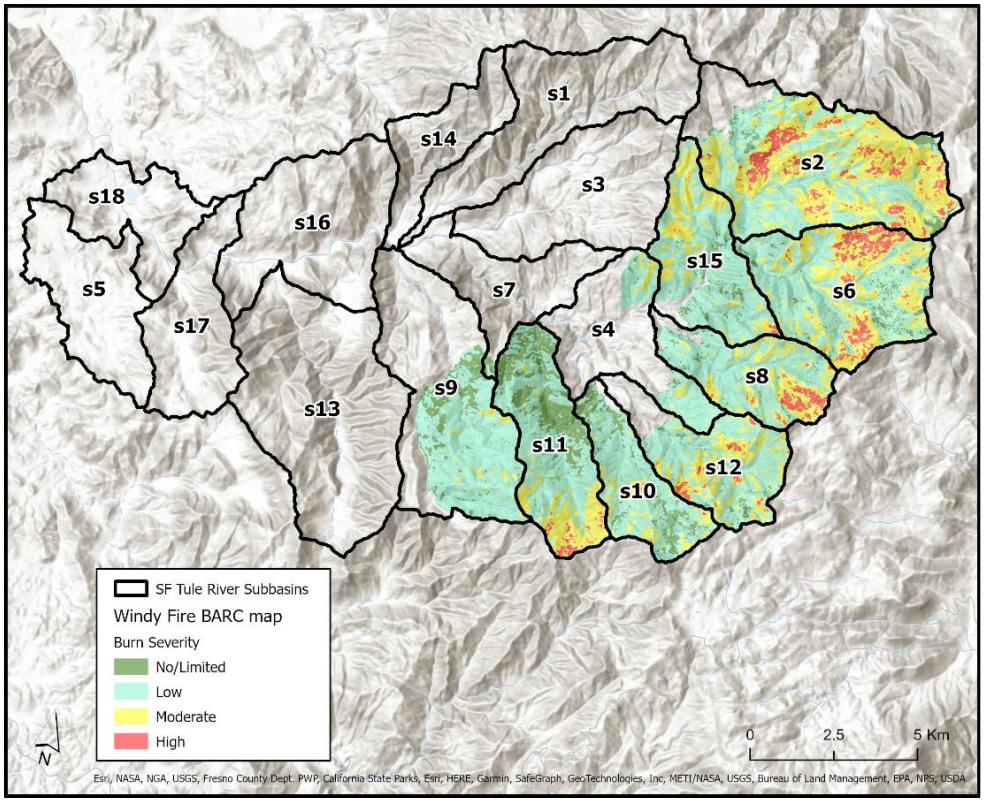

Figure 3. Detailed view of the subbasins within the Tule River watershed modeled in this study overlapped with the BARC burn severity map. Areas with no color were not burned during the fire. The green on the legend that corresponds with the BARC burn severity map also indicates areas in their study that were not burned.

The watershed area selected for this study is part of the Tule River Indian Reservation, home to over 1,000 tribal members, and spans approximately 224 square kilometers [Pritzker, 2000; SDSU]. This area is located in the heart of the San Joaquin Valley named after Tulare Lake, once the largest freshwater lake west of the Great Lakes. The outlet of the watershed was selected based on its proximity to Lake Success. The watershed has a mean basin elevation of 4,076 ft, transitioning from higher elevation at the northeast end to a lower elevation in the west, and has a total relief of 8,539 ft.

This area has all four hydrologic soil groups (HSG) present with approximately 50% of the watershed consisting of loam and clay soils (moderately high - high runoff potential) (Figure 4) (Soil Survey Staff, Web Soil Survey; SSURGO). Approximately 56% of the watershed is forested (in the east), while the western portion consists of mainly shrubs (Figure 5) (Dewitz et al, 2021). The area has a mean annual precipitation of 14 inches (Tulare County, 2022) and with the steep terrain and rapid drop in slope, these factors combine to produce the potential for significant flood events. In this region, the primary cause of floods is a result of large atmospheric rivers and related storm events (California DWR).

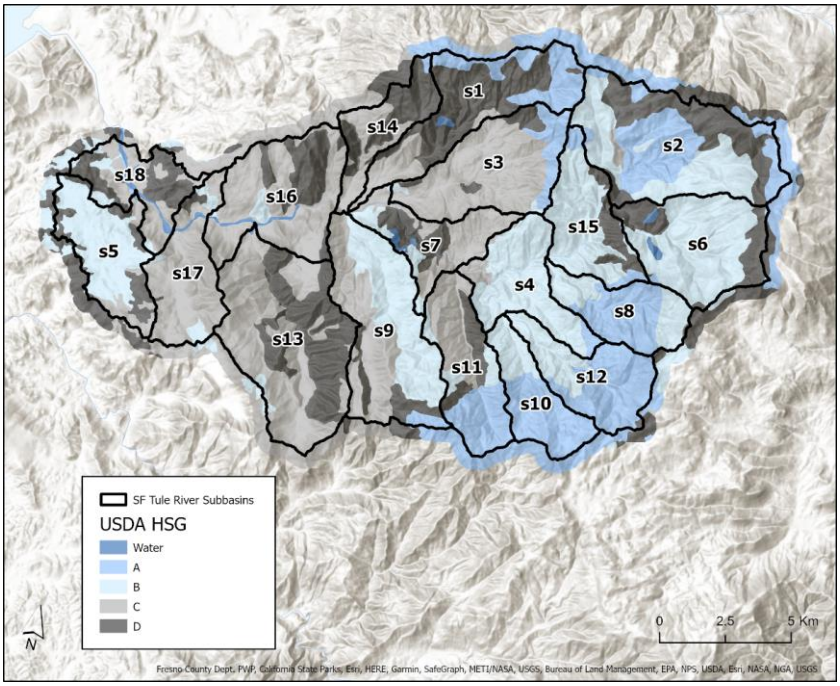

Figure 4. Soil types of the Tule River watershed modeled in this study. Hydrologic soil group (HSG) A has the lowest runoff potential (sand), HSG B has moderately low runoff potential (sandy loam, loamy sand), HSG C has moderately high runoff potential (clay loam, silty clay loam, sandy clay loam, loam, silty loam, silt), and HSG D has the highest runoff potential (clay, silty clay, sandy clay). (Soil Survey Staff, Web Soil Survey; SSURGO)

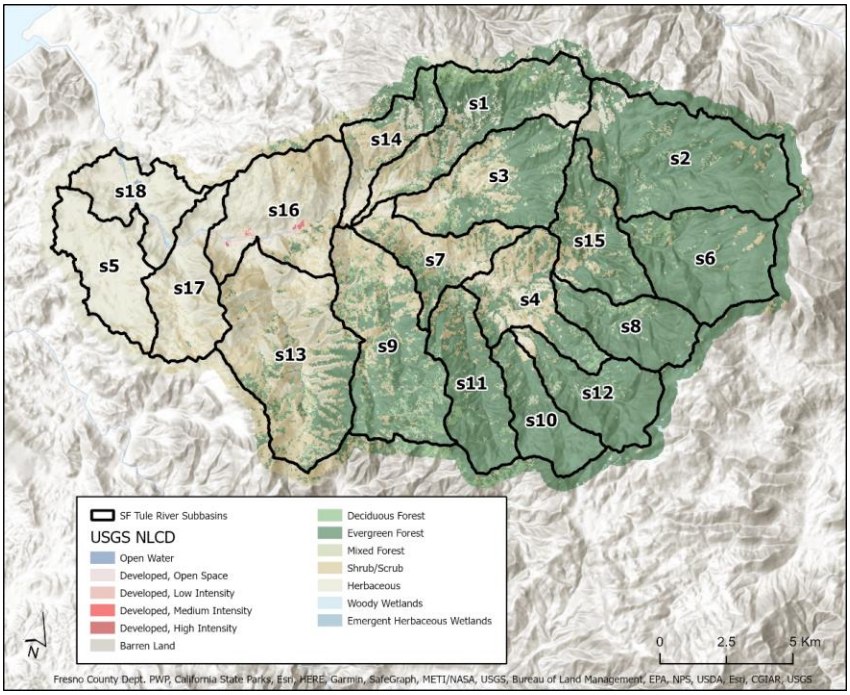

Figure 5. National Land Cover Database (NLCD) land use/land cover for the Tule River watershed modeled in this study. The majority of the land cover is forest and herbaceous. (Dewitz et al, 2021)

Methods

HEC-HMS Version 4.10 was used in this study. The model developed in this research was specifically intended to serve as a screening-level model for emergency risk assessment. It was designed in a way to provide the most accurate results in the least amount of time, therefore selected processes and methods were chosen for their simplicity and quick parameterization. All parameters were lumped at the subbasin level. The curve number method represents canopy and surface processes, and therefore these two additional methods were not utilized in the model. Furthermore, baseflow was not implemented since this is a screening-level model, however the magnitude of baseflow compared to the magnitude of the flood events is minimal and not expected to have a great impact on the results.

Loss Method

The Soil Conservation Service (SCS) Curve Number (CN) Loss Method, as described by the U.S. Department of Agriculture (USDA) Natural Resources Conservation Service (NRCS), was chosen due to the established methods for adjusting CNs for post-fire conditions, and the ease of parameterization for screening-level emergency response model development and calibration. The Curve Number loss method is an empirical method that integrates soil and land use characteristics and antecedent moisture conditions influencing runoff flow rate and volume (NRCS, National Engineering Handbook Part 630 (NEH 630), Chapter 10; USDA TR55, gNATSGO). Additional loss model parameters include the initial abstractions and percent imperviousness. The initial abstractions are calculated from the CN given the assumption inherent to the CN tables developed by the NRCS that the initial abstractions are 20% of the maximum potential retention, which is empirically related to the CN. The percent impervious is accounted for within the composite curve number, and thus is left blank.

The loss is calculated from the curve number as shown in Equation 1 through Equation 4 (NRCS, NEH 630, Chapter 10).

Equation 1: Empirical relationship between the curve number (CN) and maximum potential retention (S) in inches

$$CN = 1000/(10 + S)$$

where: S is the potential maximum retention in inches.

Equation 2: The assumed relationship between maximum potential retention (S) and the initial abstractions (I_a) in inches.

$$I_a = 0.2S$$

where: I_a is the initial abstraction in inches.

The direct runoff is then calculated as a function of the precipitation and the maximum potential retention.

Equation 3: Direct runoff volume calculation using the CN method

$$Q = (P - I_a)^2/\big((P - I_a) + S\big) = (P - 0.2S)^2/(P + 0.8S)$$

where: Q is the runoff in inches and P is the rainfall in inches.

The loss is computed at each time step by subtracting the direct runoff from the precipitation.

Equation 4: Loss calculation using the CN method

$$Loss = P - Q$$

The calibrated pre-fire CN is adjusted for post-fire conditions and serves as a surrogate for measuring changes to physical parameters that are affected by wildfire. This allows for a screening-level assessment of post-fire watershed processes without in-situ data. Most established methodologies for post-fire CN adjustment are specific to the region. However, there are currently no well-known, established methods for the area modeled in this study (USDA Forest Service Region 5). Therefore, one of the most common approaches that the BAER team utilizes to determine post-fire CNs was implemented (Table 1) (Higginson & Jarnecke, 2007).

Table 1. USDA Region 5 Curve Number Adjustment for Post-Fire Conditions

Condition	Post-fire CN Value
High Burn Severity	Calibrated Pre-fire CN + 15
Moderate Burn Severity	Calibrated Pre-fire CN + 10
Low Burn Severity	Calibrated Pre-fire CN + 5

This method directly relates the increase in CN from pre- to post-fire conditions to the BARC (Burned Area Reflectance Classification) burn severity map. The percentage of each subbasin that was burned at each burn severity was determined in ArcGIS. The CN adjustment was then applied to each of these areas and aggregated to form a composite CN at the subbasin level.

Transform Method

The SCS Unit Hydrograph Method was the selected transform method in this model (NRCS, NEH 630, Chapter 16). This method determines a hydrograph shape for each time step at each subbasin, which is additive through time based on the principle of superposition. This method requires inputs including the lag time and graph type, which determine the shape of the hydrograph.

Discharge is assumed to be linearly related to the runoff volume by a peak rate factor (PRF). The standard PRF of 484 was determined for a triangular dimensionless unit hydrograph, with the rising limb assumed to be 37.5% of the volume. The PRF can be modified to be a larger number for steeper watersheds, or a smaller number for flatter watersheds. The graph type parameter was set to the standard PRF 484 for this screening-level model.

The lag time is the delay from the time of the center of mass of excess rainfall, after losses have been removed, to when peak runoff is reached at the time of concentration. The initial lag time was computed using the Watershed Lag Method (NRCS, NEH 630, Chapter 15). The lag time is assumed to be 60% of the time of concentration, based on an empirical relationship. The time of concentration, and thus the lag time, is calculated by using the empirical relationship shown in Equation 5, which relates lag to a retardance factor, approximated as the curve number, and subbasin parameters derived from the terrain data in HEC-HMS.

Equation 5: Watershed Lag Method

$$L = (l^{0.8}(S+1)^{0.7})/(1900Y^{0.5})$$

where: L is the lag time in hours, l is the flow length in ft, Y is the average watershed land slope as a percent, and S is the maximum potential retention computed from the CN.

Routing Method

The Muskingum-Cunge (MC) method was implemented to route clear water flows in the pre- and post-fire models. Channel geometries of reach length and slope were computed by HEC-HMS's built-in geoprocessing tools. Cross section geometries were estimated from USGS site visit logs reporting flow widths, depths, and volumes. Cross section shapes were set to trapezoidal with a 1:1 side slope. High resolution cross sectional data is not essential until debris flow methods in HEC-HMS are developed to route the debris volumes through the watershed.

Debris Flow Method

The LA Debris Method EQ 2-5 was used in this study to calculate debris yield at the subbasin level (debris routing was not yet incorporated into HEC-HMS 4.10) (Gatwood et al, 2000). This method estimates debris yield as a function of drainage area, peak runoff flow, relief ratio, and a fire factor for subbasins within 3 to 200 mi^2. The user-specified fire factor is based on the percent burned and was assigned for each subbasin according to Equation 6.

Equation 6: Fire Factor according to the LA Debris Method Equation 2-5

$$Fire\ Factor = 3 * Area\ Unburned + 6.0 * Area\ Burned/Total\ Area$$

Debris flow is triggered by a Flow Rate Threshold (FRT), which is used mainly to divide storm events in continuous simulations. Since single storm events were used in this study, the FRT was simply set to 0.1. The Exponent is used to distribute the sediment load into a time-series sedigraph. A small value flattens the sedigraph compared to the hydrograph, whereas a large value heightens the sedigraph. This factor was set to 1 according to HEC guidance.

The gradation curve, which defines the distribution of the total sediment load into grain size classes and subclasses, was developed in ArcGIS Pro and Microsoft Excel using gSSURGO data from the USDA-NRCS. This data was limited and only available for 10% of the study watershed; however, it was the best available data at the time.

Input Data

The watershed was delineated with the United States Geologic Survey (USGS) StreamStats application. The digital elevation model (DEM) was obtained from the USGS National Elevation Dataset website at a resolution of 10 m (1/3 arc-second). PDS-based point precipitation frequency data was obtained from NOAA Atlas 14 (Site ID 72-0034), which ranged from 0 to 6 inches in depth depending on the frequency storm. Infiltration and available water storage were estimated from the USDA-NRCS Gridded National Soil Survey Geographic Database (gNATSGO).

Calibration and Simulation Runs

To obtain a running model quickly, the pre-fire simulation was calibrated to statistical peak flows at USGS gage 11204500. A separate basin model was created for each AEP event (1/1, 1/10, 1/25, 1/100) to represent low, moderate, and high system dynamics. Each model was calibrated independently by adjusting the CNs and lag times by a constant factor until the computed peak flow matched the statistical peak flow. The constant factors increased as the AEP event increased in severity, which resulted in higher CNs and lag times for the larger storms. There was no available data for post-fire conditions, thus the model was only calibrated for pre-fire conditions and the post-fire CNs were adjusted as described above. The 1/10, 1/25, and 1/100 AEP floods were run for both pre- and post-fire models. These storms consisted of a 6-hour duration, 5-minute intensity duration, and a 50 percent intensity position. The TP40/TP49 Area Reduction was applied and the spatial distribution was uniform for all subbasins. Simulations were run over a period of one day.

Results

As HEC-HMS's current Debris Flow Library provides static (un-routed) sediment volumes at the subbasin level, the analysis was performed for individual subbasins. This included Subbasins 2, 6, 9, and 10 which were chosen based on their burn conditions (Table 2). Subbasin 9 had a relatively small percentage of total burn, Subbasin 10 had the highest percentage of low burn, Subbasin 2 had the highest percentage of medium (and high) burn, and Subbasin 6 had the highest percentage of high burn (in addition to Subbasin 2) as well as the highest percentage of total burn.

Table 2. Burn percentage and burn severity breakdown for the four subbasins analyzed in this study

		Burn Percentage			
	Area (mi²)	Low	Medium	High	Total
Subbasin 2	10.8	35%	40%	9%	84%
Subbasin 6	7.0	51%	34%	9%	94%
Subbasin 9	9.1	40%	2%	0%	42%
Subbasin 10	3.7	66%	15%	0%	81%

Figures 6 through 9 show the excess precipitation hyetographs and hydrographs for pre-fire events with sedigraph results included for the post-fire events. Graphs are included only for the highest burned subbasin (largest percentage of high and medium burn severity) and least burned subbasin for the sake of report brevity.

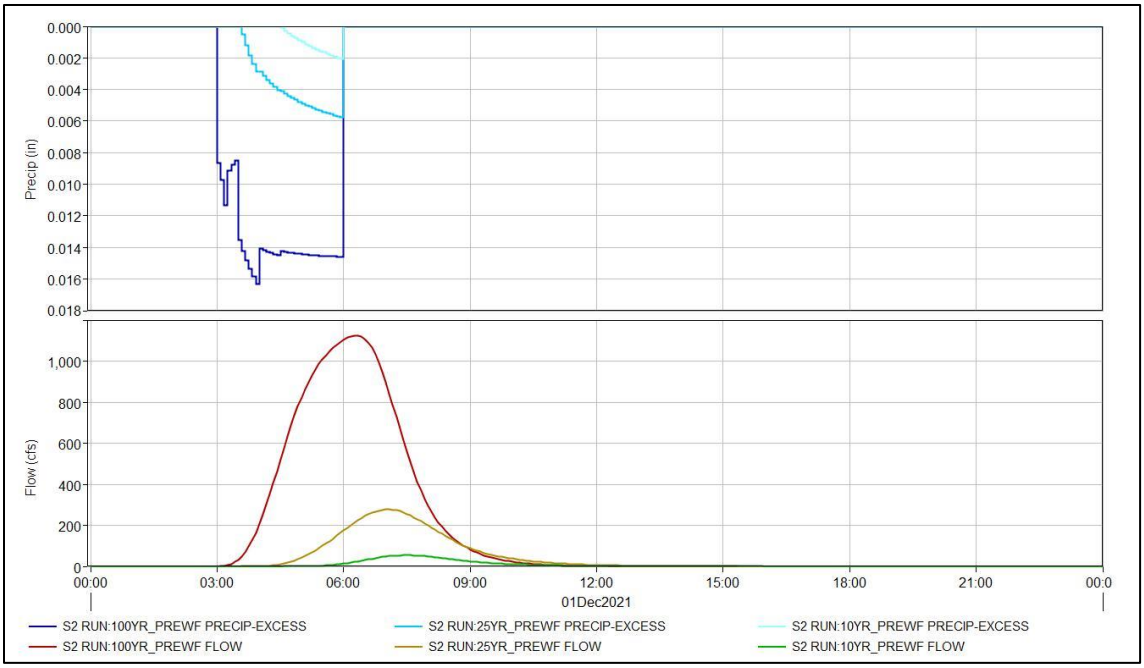

Figure 6. Excess precipitation (top) and discharge (bottom) for Subbasin 2 under pre-fire conditions for the 1/100, 1/25, and 1/10 AEP floods (100-, 25-, and 10-year frequency storms). Note, the excess precipitation is practically zero in this pre-fire condition, because most of the precipitation is infiltrating into the ground.

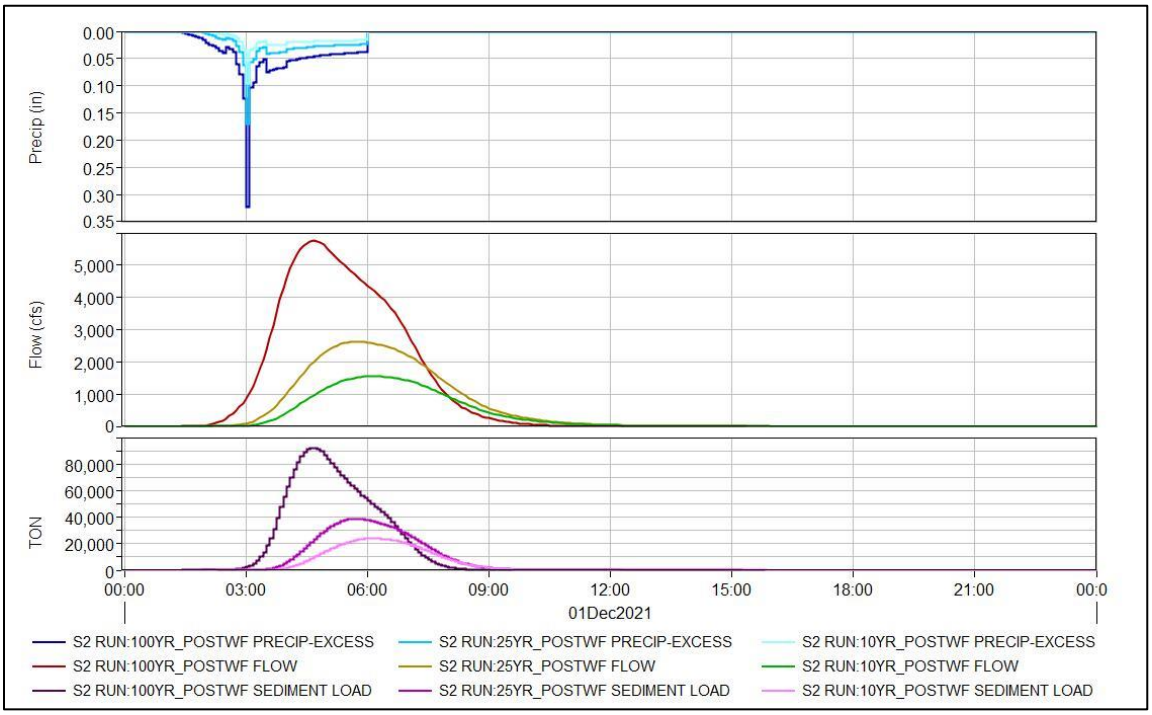

Figure 7. Excess precipitation (top), discharge (middle), and sediment load (bottom) for Subbasin 2 under post-fire conditions for the 1/100, 1/25, and 1/10 AEP floods (100-, 25-, and 10-year frequency storms). Note, the excess precipitation has increased in this post-fire condition due to a decrease in infiltration capacity after the fire.

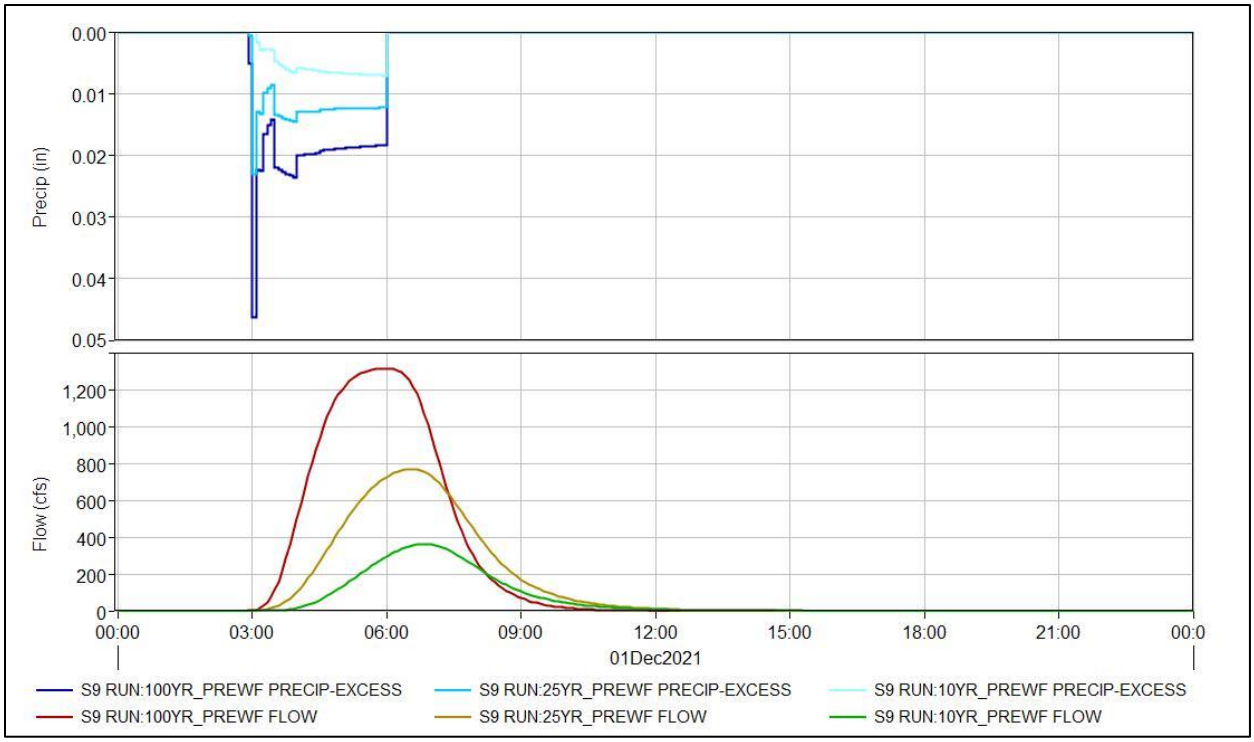

Figure 8. Excess precipitation (top) and discharge (bottom) for Subbasin 9 under pre-fire conditions for the 1/100, 1/25, and 1/10 AEP floods (100-, 25-, and 10-year frequency storms).

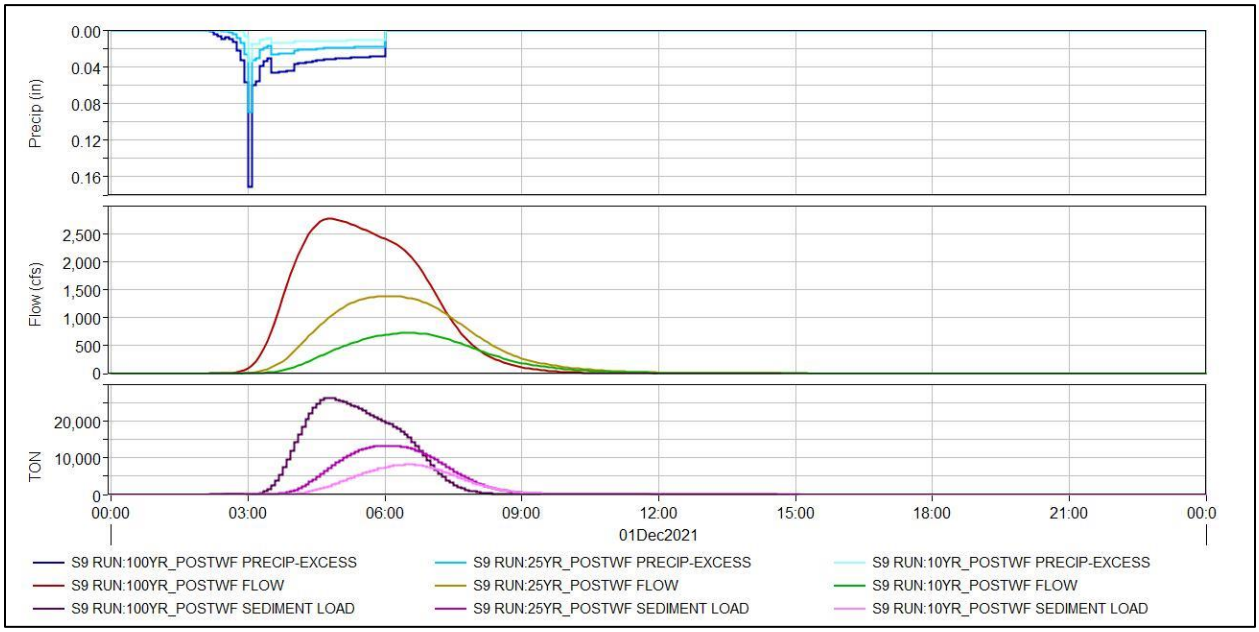

Figure 9. Excess precipitation (top), discharge (middle), and sediment load (bottom) for Subbasin 9 under post-fire conditions for the 1/100, 1/25, and 1/10 AEP floods (100-, 25-, and 10-year frequency storms).

Figure 10 shows the pre- and post-fire difference in peak discharge for each subbasin. Subbasin 2, which had the highest medium burn severity percentage at 40% and highest high burn severity at 9%, experienced the highest difference in peak discharge. The 1/25 AEP flood (25-year storm) resulted in a difference of approximately 2,360 cfs for this subbasin. Subbasin 6, which also had a high burn severity of 9% as well as the highest percentage of overall burn at 94%, had similar results with a difference in peak discharge of about 1,760 cfs for the 1/25 AEP flood. Subbasins 9 and 10, which had the lowest overall burn percentage at 42% and highest percentage of low burn severity at 66%, respectively, yielded similar results with a difference in peak discharge of approximately 610 cfs and 450 cfs for the 1/25 AEP flood.

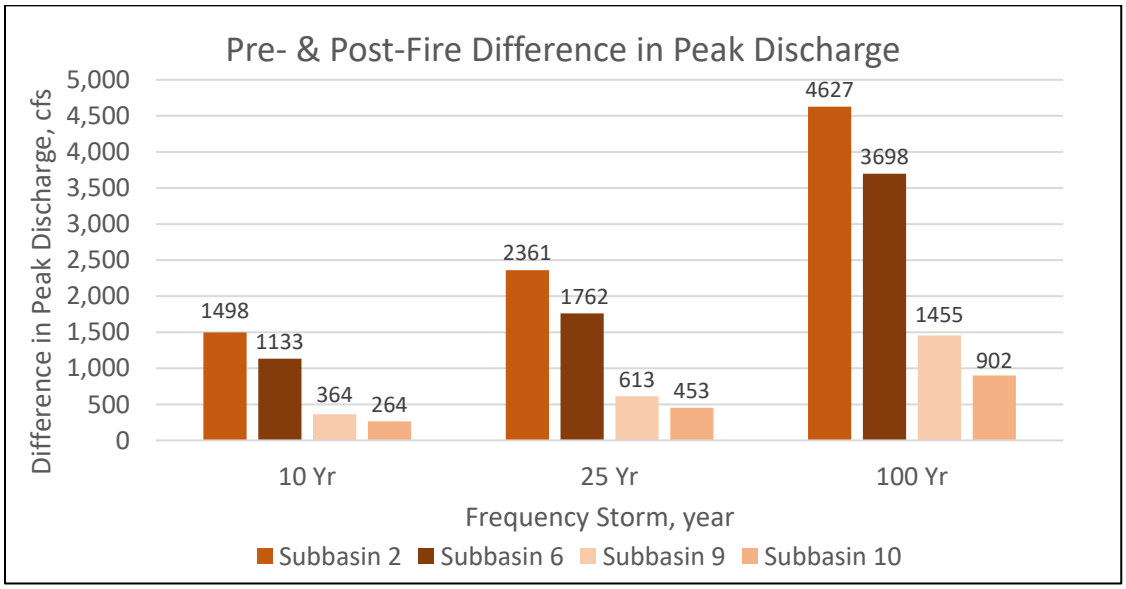

Figure 10. Difference in peak discharge between pre- and post-fire conditions for Subbasins 2, 6, 9, and 10. The 10-yr, 25-yr, and 100-yr storms correlate to the 1/10, 1/25, and 1/100 AEP floods, respectively.

Figure 11 shows the pre- and post-fire percent difference in peak discharge for each subbasin, which was calculated by dividing the absolute value of the difference by the average of the two values. For the 1/25 AEP flood, Subbasins 2, 6, and 10 yielded similar percent differences in peak discharge of approximately 160%, 150%, and 150%, respectively. Subbasin 9, which had the lowest percentage of overall burn at 42%, experienced a percent difference in peak discharge of about 60%.

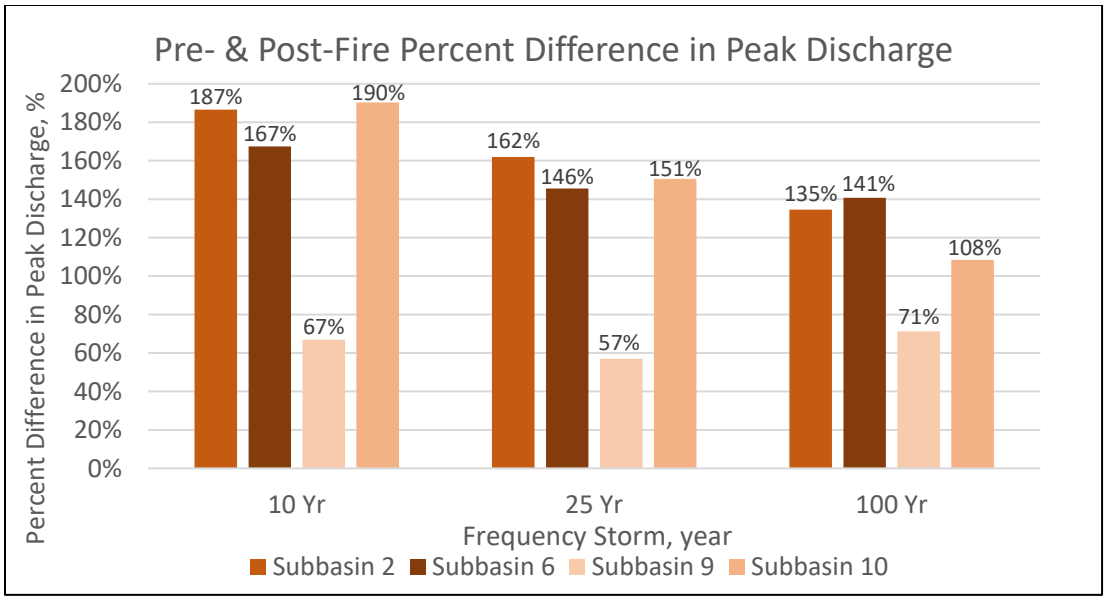

Figure 11. Percent difference in peak discharge between pre- and post-fire conditions for Subbasins 2, 6, 9, and 10. The 10-yr, 25-yr, and 100-yr storms correlate to the 1/10, 1/25, and 1/100 AEP floods, respectively.

Figure 12 shows the post-fire sediment load for each subbasin. Sediment yield for the highest burned subbasins after the 1/100 AEP flood is notably larger than the other two storms. Subbasin 6, which tied for the highest percentage of high burn severity and had the largest percentage of total burn, resulted in the largest sediment yield for all three storms, which was approximately 126,000 tons for the 1/100 AEP flood and 52,000 tons for the 1/25 AEP flood. It is interesting to note that Subbasin 2, which had an equivalent percentage of high burn severity and the largest percentage of medium to high burn severity, resulted in a smaller sediment yield than Subbasin 6. This illustrates that the higher percentage of area that was burned at a low burn severity in Subbasin 6 contributed to a higher sediment yield compared to Subbasin 2, which experienced a smaller area of low burn.

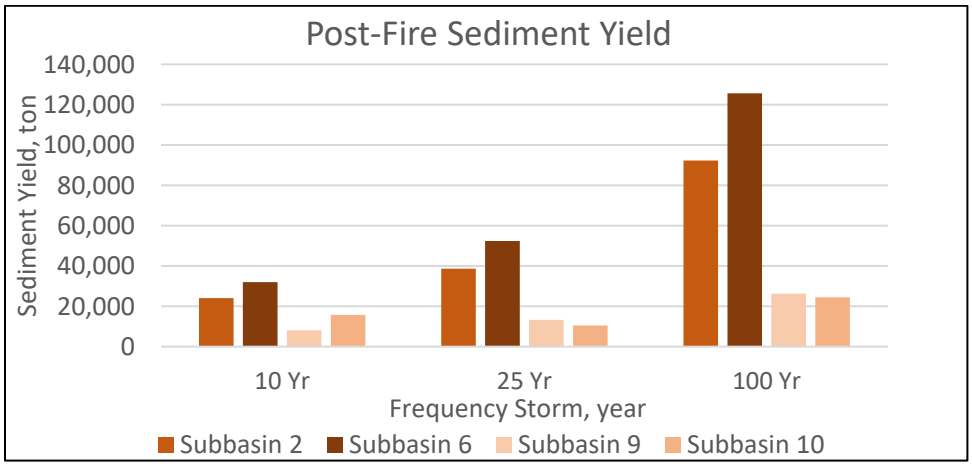

Figure 12. Post-fire sediment load for Subbasins 2, 6, 9, and 10. The 10-yr, 25-yr, and 100-yr storms correlate to the 1/10, 1/25, and 1/100 AEP floods, respectively.

Conclusion

A screening-level HEC-HMS model was developed to estimate post-fire runoff in the Tule River watershed as part of a larger research task to identify the simplest and most accurate methods for developing a post-fire runoff model in emergency risk assessments. Due to the short timeframe for these type of assessments, quick model parameterization and calibration is crucial and thus, was the approach for this model development. The SCS Curve Number and SCS Unit Hydrograph methods were used to develop and calibrate the pre-fire model. Curve numbers were modified for post-fire conditions and debris yield was estimated with the LA Debris EQ 2-5.

Subbasins with the highest overall burn percentage (S6 & S2) resulted in larger differences between pre- and post-fire peak discharges compared to subbasins that experienced a smaller burn percentage, as anticipated. For example, the percent difference in peak discharge for the 1/25 AEP flood for the highest burned subbasin (S6) and the least burned subbasin (S9) was 146% and 57%, respectively. This trend was also clear in the debris yield results. For the 1/25 AEP flood, Subbasin 6 yielded approximately 52,000 tons of sediment while Subbasin 9 yielded 13,000 tons. Sediment yields for the 1/10 and 1/25 AEP floods were relatively close in contrast to the 1/100 AEP flood, which increased dramatically for the higher burned subbasins. For example, Subbasin 2 resulted in a sediment yield of 39,000 and 24,000 tons for the 1/25 and 1/10 AEP floods, respectively, while it resulted in 92,000 tons for the 1/100 AEP flood. This is most likely due to the fact that the debris yield equation that was used is based on peak discharge, which increases drastically between the 1/25 AEP flood (2,360 cfs) and the 1/100 AEP flood (4,630 cfs). Perhaps the most interesting finding is that peak discharges were highest for Subbasin 2 while sediment yields were highest for Subbasin 6. Subbasin 2 had a higher percentage of medium to high burn severity and resulted in larger peak flows, whereas Subbasin 6 had a higher percentage of low burn severity, and therefore total burn percentage, which resulted in higher sediment yields. This is likely due to either the difference in burn severity and overall burn percentage, or the transfer from debris flow Equation 2 to Equation 3, which is triggered based on subbasin size (Equation 2 is used for subbasins between 3 and 10 mi^2 and Equation 3 is used for subbasins between 10 and 25 mi^2) (Gatwood et al, 2000). This could be an interesting topic for further research.

Simplifying several methods was necessary to reduce the development period for screening level model production. Future improvements to the screening-level model workflow are suggested to improve accuracy of results. Straightforward improvements include exercising the optimization methods in HEC-HMS for calibration and using a distributed precipitation frequency grid instead of a single rain gage. Improvements that are more complex include calibrating the pre-fire model to observed events rather than statistical peak flows and performing a sensitivity analysis to improve understanding of model results. In addition to this, any processes that could be transitioned from lumped (averaged) to distributed would also improve model accuracy. However, the most critical factor for model improvement is post-fire data. Until this is acquired, the model can only be calibrated to pre-fire conditions and results should be taken with a grain of salt (or sediment). As these improvements are implemented and calibration data from the field is integrated, screening-level results will continue to improve.

REFERENCES

Berger, Noah. 2021. Associated Press. Los Angeles Times. “Four Guardsmen safe, but giant sequoia burns; cabins threatened.” https://www.latimes.com/california/story/2021-09-21/windy-fire-burns-giant-sequoia-as-knp-complex-nears-cabins.

Dewitz, J., and U.S. Geological Survey, 2021, National Land Cover Database (NLCD) 2019 Products (ver. 2.0, June 2021): U.S. Geological Survey data release, https://doi.org/10.5066/P9KZCM54.

Gatwood, E., Pedersen, J, Casey, K., 2000. Los Angeles District Method for Prediction of Debris Yield. U.S. Army Corps of Engineers, Los Angeles District, Los Angeles, California, pp. 1-20. http://www.spl.usace.army.mil/resreg/htdocs/DebrisMethod.pdf.

Higginson, B., Jarnecke, J. 2007. Salt Creek BAER-2007 Burned Area Emergency Response. Provo, UT: Unita National Forest, Hydrology Specialist Report.

Inciweb. Windy Fire. https://inciweb.nwcg.gov/incident-maps-gallery/casqf-windy-fire. Accessed 15 December 2022.

NOAA Atlas 14 Precipitation Frequency Data Server. https://hdsc.nws.noaa.gov/hdsc/pfds/pfds_map_cont.html

NRCS, National Engineering Handbook, Part 630 Hydrology. *Hydrologic Soil-Cover Complexes*. Chapter 9. https://directives.sc.egov.usda.gov/OpenNonWebContent.aspx?content=17758.wba

NRCS, National Engineering Handbook, Part 630 Hydrology. *Estimation of Direct Runoff from Storm Rainfall*. Chapter 10. https://directives.sc.egov.usda.gov/17752.wba

NRCS, National Engineering Handbook, Part 630 Hydrology. *Time of Concentration*. Chapter 15. https://directives.sc.egov.usda.gov/27002.wba

NRCS, National Engineering Handbook, Part 630 Hydrology. *Hydrology*. Chapter 16. https://directives.sc.egov.usda.gov/17755.wba

Pritzker, Barry M. *A Native American Encyclopedia: History, Culture, and Peoples*. Oxford: Oxford University Press, 2000. ISBN 978-0-19-513877-1

SDSU Library and Information Access. *California Indians and Their Reservations*. Accessed 25 November 2022.

Soil Survey Staff, Natural Resources Conservation Service, United States Department of Agriculture. Web Soil Survey. Available online at the following link: *http://websoilsurvey.sc.egov.usda.gov/*. Accessed 14 December 2022.

Soil Survey Staff, Natural Resources Conservation Service, United States Department of Agriculture. Soil Survey Geographic (SSURGO) Database for [California]. Available online. Accessed 14 December 2022.

Tulare County Economic Development Corporation. *Climate*. https://www.tularecountyedc.com/living-here-2/climate/. Accessed 14 December 2022.

USDA Gridded National Soil Survey Geographic Database (gNATSGO). https://www.nrcs.usda.gov/wps/portal/nrcs/detail/soils/survey/geo/?cid=nrcseprd1464625

USDA TR55. *Urban Hydrology for Small Watersheds*. https://nationalstormwater.com/wp/wp-content/uploads/2020/07/Urban-Hydrology-for-Small-Watersheds-TR-55.pdf

USGS National Elevation Dataset. https://www.usgs.gov/programs/national-geospatial-program/national-map

USGS StreamStats: Streamflow Statistics and Spatial Analysis Tools for Water-Resources Applications. https://streamstats.usgs.gov/ss/